
B²EA: An Evolutionary Algorithm Assisted by Two Bayesian Optimization Modules for Neural Architecture Search

Hyunghun Cho
GSCST,
Seoul National University
webofthink@snu.ac.kr

Jungwook Shin
GSCST, Seoul National University
& SK Telecom Co., Ltd.
jungwook.shin@snu.ac.kr

Wonjong Rhee
GSCST & GSAI & AIIS,
Seoul National University
wrhee@snu.ac.kr

Abstract

The early pioneering Neural Architecture Search (NAS) works were multi-trial methods applicable to any general search space. The subsequent works took advantage of the early findings and developed weight-sharing methods that assume a structured search space typically with pre-fixed hyperparameters. Despite the amazing computational efficiency of the weight-sharing NAS algorithms, it is becoming apparent that multi-trial NAS algorithms are also needed for identifying very high-performance architectures, especially when exploring a general search space. In this work, we carefully review the latest multi-trial NAS algorithms and identify the key strategies including Evolutionary Algorithm (EA), Bayesian Optimization (BO), diversification, input and output transformations, and lower fidelity estimation. To accommodate the key strategies into a single framework, we develop B²EA that is a surrogate assisted EA with two BO surrogate models and a mutation step in between. To show that B²EA is robust and efficient, we evaluate three performance metrics over 14 benchmarks with general and cell-based search spaces. Comparisons with state-of-the-art multi-trial algorithms reveal that B²EA is robust and efficient over the 14 benchmarks for three difficulty levels of target performance. The B²EA code is publicly available at <https://github.com/snu-ads1/BBEA>.

1 Introduction

The historical success of AlexNet [38] triggered an exploding interest in deep learning and identification of high-performance neural architectures emerged as a crucial task. As the manual search continued as the dominant approach, the importance of automatic Neural Architecture Search (NAS) has become evident. The early works focused on traditional Hyper-Parameter Optimization (HPO) methods such as Bayesian Optimization (BO) [59, 33, 7], where the search space was general and included both basic hyperparameters (e.g., learning rate, regularization parameters [59]) and partial architectural elements (e.g., number of neurons in a layer, filter size, pooling option [6]). Following the early efforts, intensive architecture search was performed over entire-structured search spaces [71, 3, 54] where neural architectures achieving state-of-the-art performance were discovered at the cost of a substantially large computation. To reduce the computational burden, the research community quickly moved into a new paradigm where NAS algorithms focus on special search spaces such as cell-based, hierarchical, or morphism-based [30], where pre-fixed hyperparameters are used. The most recent studies, however, recognized several downsides of the new paradigm and it is becoming apparent that a few distinct types of NAS algorithms are needed [42, 12, 63].

NAS methods can be categorized in a few different ways, and comprehensive surveys were provided by Elsken et al. [21] and He et al. [30]. An essential factor is the number and type of training that

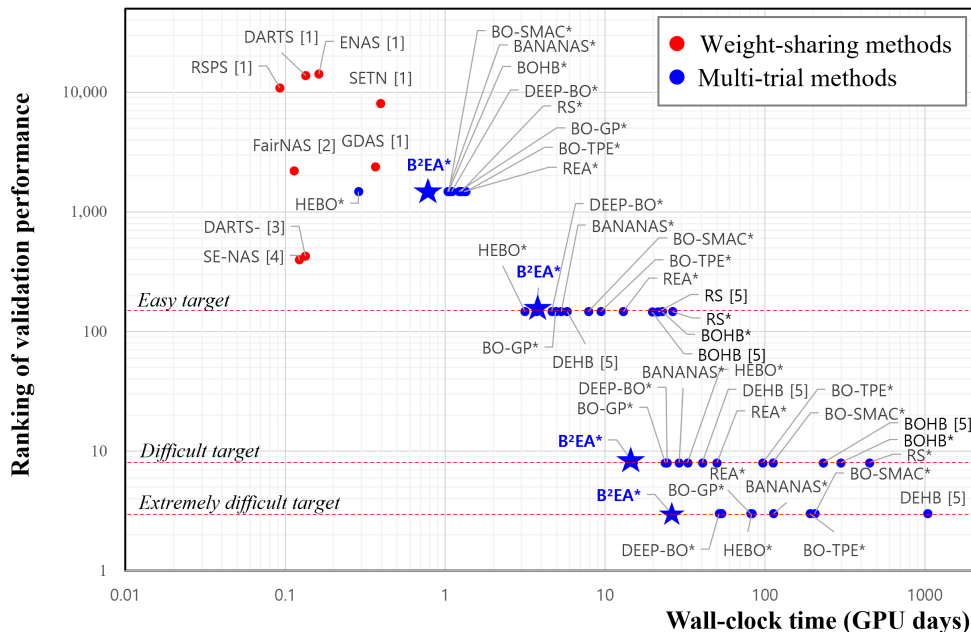


Figure 1: Comparison of NAS methods for NAS-Bench201-ImageNet16-120 task. Algorithm names with * indicate the evaluation results of this work. The results reported in five existing works are shown together: [1] Dong & Yang [18], [2] Chu et al. [13], [3] Chu et al. [11], [4] Hu et al. [32], and [5] Awad et al. [2].

needs to be performed to complete a search because they directly affect the computational burden. *One-shot* NAS trains an overparameterized supernet, and considers only the subnets as the search space [8, 4, 69, 28, 32]. Repeated full training can be avoided in this way, and Liu et al. [47] showed that efficient gradient descent methods can be utilized with a proper search space design. Some of the previous studies reported that one-shot methods can cause instability problems in practice [68, 11, 63]. Dong et al. [19] divides NAS methods into *weight-sharing* and *multi-trial*. Weight-sharing includes not only differentiable methods but also other approaches that utilize the concepts like sharing weights between models [8, 53] and progressive training [34, 45]. Multi-trial methods perform multiple full training over different configurations, and it is often believed that multi-trial requires a prohibitive computational cost. Multi-trial, however, is known to excel at identifying very high-performance architectures while weight-sharing can fail to do so.

In Figure 1, performance of NAS methods is shown for ImageNet16-120 task in NAS-Bench201 [18]. The benchmark contains a total of 15,625 candidate configurations. The ranking of the neural architecture search result is shown because accuracy or error rate can be misleading depending on the performance distribution over the candidate configurations. For our results that are marked with *, the average performance was calculated over 500 runs with random seeds. NAS-Bench201-ImageNet16-120 is one of the 14 benchmarks that we study in this work, and its search space is cell-based. Therefore, it is possible to show the results of weight-sharing methods together. Note that most of the weight-sharing or one-shot methods cannot be evaluated for the benchmarks with a general search space (e.g., benchmarks in HPO-Bench [36] and DNN-Bench [9]).

The one-shot methods marked with [1] in Figure 1 (RSPS [42], DARTS [47], ENAS [53], SETN [16], GDAS [17]) show poor performance. The cell design of NAS-Bench201 includes skip-connection and the difference in search space is known to be the reason of the performance degradation [63]. Recent robustified methods marked with [2],[3], and [4] perform better, and DARTS- [11] and SE-NAS [32] achieve the best performance for the category of search budget below one GPU day. When the search budget is larger and a search for a high-performance architecture is desired, however, clearly multi-trial NAS algorithms can be imperative.

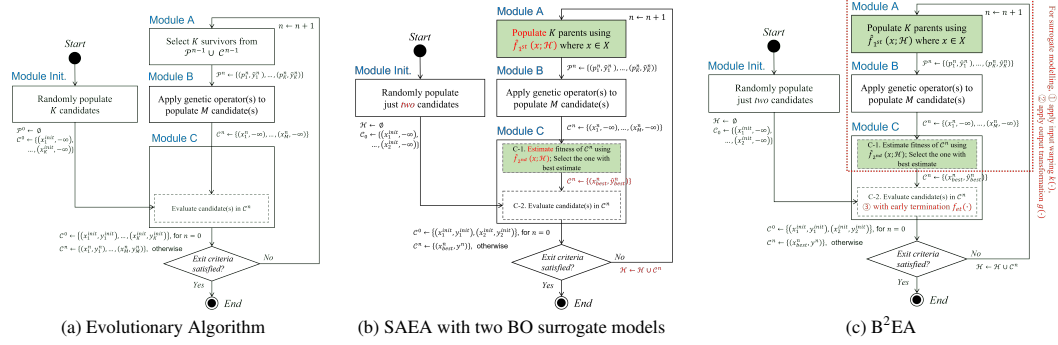


Figure 2: Process flow diagrams of (a) basic EA, (b) enhanced EA with two BO surrogate models, and (c) further enhanced EA (B^2EA) with an input warping strategy $k(\cdot)$, an output transformation strategy $g(\cdot)$, and a conservative early termination strategy $f_{et}(\cdot)$.

In this study, we develop a multi-trial NAS algorithm that can be useful when searching for a high-performance architecture or when the search space is general. Our algorithm is named as B^2EA where the name comes from the use of two Bayesian Optimization (BO) surrogate models within an Evolutionary Algorithm (EA). For the ‘*Difficult target*’ in Figure 1, it can be seen that our algorithm can complete the search within 15 GPU days while random search (RS) needs around 450 GPU days. The process flow diagram of an EA is shown in Figure 2a. While EA is a search method, it has an interesting analogy with the three dimensions of NAS that were identified by Elsken et al. [21] - *search space*, *search method*, and *evaluation method*. In Figure 2a, Module A performs the role of controlling *search space* and Module C performs the role of *evaluating* the selected candidate(s). This inspired us to adopt two BOs as shown in Figure 2b and to come up with a new type of Surrogate Assisted Evolutionary Algorithm (SAEA) [35]. The first BO in Module A is responsible for adaptively controlling the search space. The second BO in Module C is used for estimating the performance of many candidate configurations without any DNN training. To our best knowledge, this is the first time to have two BO models used together with an EA. While several options are available for the genetic operator in Module B, we choose mutation because it is simple and can complement BO models that can become biased [51]. Besides the main idea of combining two BO surrogate models and an EA, B^2EA embraces three key strategies from the latest works as shown in Figure 2c.

2 Related works

EA and BO: For the conventional black-box optimization problems, Evolutionary Algorithm (EA) has been favored for the functions with cheap evaluation costs while Bayesian Optimization (BO) has been preferred for the functions with expensive evaluation costs. EA tends to provide a robust performance over a wide variety of optimization tasks, but it requires a large number of function evaluations. BO tends to be an efficient solution in terms of computational burden, but it works well only if the choice of modeling happens to match the problem characteristics and also a catastrophic modeling bias does not occur [9]. While the early NAS works often considered BO as the search method, the extremely high cost of deep neural network training discouraged researchers from studying EA. Surprisingly, however, a simple EA method known as REA [55] has been shown to be effective for automatically designing neural architectures and surpassed the performance of human designs [54].

SAEA: Surrogate-assisted evolutionary algorithm (SAEA) is a subclass of EA, where a surrogate model is used to augment the prediction of fitness during the search. The motivation of SAEA is to reduce the function evaluation cost of the expensive problems [35]. A surrogate model can be used for offspring generation [22] or for lazy evaluation [49]. In the EA community, typically SAEA works have been evaluated with synthetic object functions known as COCO benchmark [29]. In our work, the target application of multi-trial NAS is distinct because of the exceptionally high cost of function evaluation. Compared to the computational cost of a full DNN training, the computational cost of surrogate modeling becomes negligible. This is one of our motivations for adopting two BO surrogate models into B^2EA .

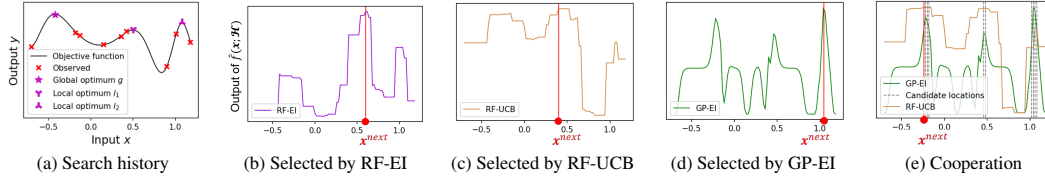


Figure 3: Enhancement through cooperation. An optimization problem with one-dimensional search space is shown in (a), where nine candidates have been evaluated so far. Global and local optima are shown as well. Compared to the individual decisions in (b), (c), and (d), a cooperative decision can lead to a better candidate selection, as shown in (e). The cooperation is achieved by the first BO model (GP-EI in this example) constraining the search space to its top $M=10$ points and the second BO model (RF-UCB in this example) choosing its best only from these M candidate points. Because the two models have different modeling characteristics, they end up compromising on the final candidate selection.

Input and output transformations: HEBO is the winner of the black-box optimization (BBO) challenge at NeurIPS 2020 [61], where the challenge focused on evaluating derivative-free optimizers for tuning the hyperparameters of machine learning models. To deal with the complexities associated with the competition datasets, both input and output nonlinear transformations were used [14]. More specifically, they utilized an input warped GP [60] to handle non-stationary functions and output transformations [56] to model non-Gaussian data. DEEP-BO also utilizes an output transformation and explains it as one of the four basic BO enhancement strategies [9]. In our work, we integrate input warping and output transformation as in HEBO.

Multi-fidelity: While multi-fidelity techniques [15, 23] are becoming popular, they have been underutilized in the NAS community [66]. This is because the estimation of validation performance based on lower fidelity observations can be inaccurate [25, 21]. For instance, it has been pointed out that the use of batch-norm can cause a large gap between a low fidelity observation based estimation and the corresponding high fidelity evaluation [10, 9]. For B²EA, we choose to stay conservative and integrate the *early termination rule* [9] that is known to have a minimal influence on NAS performance, especially when searching for an architecture of high performance.

3 Cooperation between two BO models

Before moving forward, we explain the key design concepts of B²EA’s two BO surrogate models.

Diversified BO: While BO can be an efficient strategy even when the cardinality of search history $|\mathcal{H}|$ is small, it can also be biased and catastrophic. A typical BO can be myopic because it considers no more than a single step in the future [26], and its common acquisition functions can lead to an overly greedy optimization [58]. To address this drawback of BO, we adopt a diversified BO [9]. Diversified BO relies on multiple BO models, as in the ensemble, and it can escape from a local optimum simply by rotating over a set of BO models. Once an informative sample is added to the search history \mathcal{H} , the previously catastrophic models can become effective as well. Because adaptive diversification was shown to be not so helpful in Cho et al. [9], we adopt round-robin diversification for the first BO module and uniform random diversification for the second BO module. An example of catastrophic behavior can be found in Figure S2 of Supplementary D.

Cooperation between two BO surrogate models: In Figure 2b, the first BO, \hat{f}_{1st} , is responsible for dynamic adjustment of the search space and the second BO \hat{f}_{2nd} is responsible for the performance estimation of the M candidates. While the two modules have been designed for two distinct goals, they can also be understood as a group. In Figure 3, it can be seen that the first BO’s candidate selections are regularized by the second BO, which has a different opinion from the first BO. In addition to the diversification of BO, this cooperation plays a key role in making B²EA robust over a variety of optimization tasks.

4 Proposed method: B²EA

Compared to the weight-sharing NAS algorithms, multi-trial NAS algorithms require far more computational time. This means a failed search can be much more painful for a multi-trial NAS. Therefore, we have chosen *robustness* over a broad range of complicated black-box optimization problems as the most important goal when developing B²EA. To achieve high robustness while relying on BO for computational efficiency, we adopt three strategies - diversification at a single BO level, cooperation at multiple BO level, and mutation at EA level. In this section, we first explain the SAEA framework that implements the three robustness strategies and then briefly explain the additional enhancement strategies.

4.1 SAEA framework

The insights behind B²EA includes dynamic search space control with the first diversified BO and cheap function output estimation with the second diversified BO. The process flow diagram of B²EA is shown in Figure 2c, and the pseudo-code is shown in Algorithm S1 of Supplementary B. The main steps of Algorithm S1 can be explained as follows:

Initialization: For the basic EA in Figure 2a, the initial population C^0 consists of randomly selected K candidates. This simple initialization scheme poses two main problems for functions with high evaluation costs. First, all K candidates must be evaluated. Second, the random selection of K candidates can be highly inefficient from BO’s perspective because BO can perform much better by sequentially selecting the K candidates. Therefore, we modify the initialization step of EA to choose only two candidates \mathbf{x}_1^{init} and \mathbf{x}_2^{init} as is usually done in BO. For a typical BO with a continuous search space, one candidate is chosen near the center, and the other is chosen near the boundary corner. In our implementation, however, we have randomly chosen the two candidates because some of the search dimensions are not continuous and it can be ambiguous to identify near-center or near-boundary candidates.

Module A: For the genetic algorithm, which is a type of EA, optimization is performed over many generations, and the building-block hypothesis is often believed to be the reason for its frequent success. In the building-block hypothesis, “*short, low order, and highly fit schemata are sampled, recombined, and resampled to form strings of potentially higher fitness*” [24]. In Figure 2a, the population in module A is iteratively updated using tournaments or other methods for selecting the survivors, and the population is expected to retain highly fit schemata as it evolves. Traditional EA methods [70, 55] have a strategy to remove some candidates in \mathcal{P}^n in consideration of limited computational resources. In contrast, B²EA dynamically generates a fresh set of K candidates for each iteration n using the first diversified BO \hat{f}_{1st} . The history \mathcal{H} is used for modeling \hat{f}_{1st} , and the top K performing candidates from the search space \mathcal{X} are chosen based on the performance estimates of \hat{f}_{1st} . In this way, we are giving up on the building block hypothesis that may take a long time to be effective, and instead relying on the modeling capability of the BO, which can be useful even with a small number of evaluated candidates. Because diversified BO can be highly accurate even when $|\mathcal{H}|$ is small, this replacement can be a key enhancement factor for functions with high evaluation costs.

Module B: We keep the basic functionality of the EA’s genetic operation intact, but we consider only mutation in this work. There are many other possibilities, for instance, crossover or mutation followed by crossover. However, our main interest is to investigate the benefits and robustness of integrating two diversified BO modules into a basic EA framework, and thus we intentionally keep this part simple. In Figure 2b, module B is responsible for generating M candidates to form C^n by applying mutation to the K parents in \mathcal{P}^n . Assuming $K \geq M$ for simplicity, B²EA randomly selects M candidates from \mathcal{P}^n with a mutation applied to a randomly selected dimension of \mathbf{x} for each candidate to generate M offsprings that form C^n . We follow the intensification strategy of Hutter et al. [33] to handle mixed-type hyperparameters.

Module C: For the basic EA in Figure 2a, module C simply evaluates all M candidates. Obviously, this is not desirable for functions with high evaluation costs, including NAS. To alleviate this problem, we use the second BO module \hat{f}_{2nd} to cheaply estimate the true function values of the M candidates. Upon completion of the estimation, the candidate with the best estimate is chosen as the final candidate and its true function value is evaluated. In an extreme scenario, modules A and B can be configured such that the entire search space \mathcal{X} is contained in C^n . In this case, modules A and B do

Table 1: Tabular benchmarks for NAS

Benchmark name	Number of tasks			Number of hyperparameters						Full candidate set size
	MLP	CNN	RNN	Categorical	Continuous	Discrete	$ \mathbf{x}_A $	$ \mathbf{x}_H $	$ \mathbf{x} $	
HPO-Bench	4	-	-	3	3	3	4	5	9	62,208
NAS-Bench-101	-	1	-	5	-	21	26	-	26	423k
NAS-Bench-201	-	3	-	6	-	-	6	-	6	15,625
DNN-Bench	-	5	1	0~3	2~5	2~6	1~7	3~7	7~10	20,000†

†Except for CIFAR10-ResNet, which has 7,000 configurations.

not perform any meaningful operation, and the entire EA framework collapses to a BO algorithm (module C only). In this sense, B²EA can be considered as a class of algorithms that include BO as a subclass.

Exit criteria and update of \mathcal{H} : Exit criteria are configured in the same manner as in any EA or BO algorithm. In our experiments, we consider fixed budget targets and fixed performance targets. History \mathcal{H} is updated by adding $(\mathbf{x}_{best}^n, \mathbf{y}^n)$, as in any BO.

4.2 Further enhancements

Besides the main development of SAEA with two BO surrogate models, we adopt input warping [60] and output transformation [56] as in HEBO. Also, we adopt the early termination rule [9] from DEEP-BO. The resulting B²EA is shown in Figure 2c.

5 Experiments

We evaluate three NAS benchmark datasets that are publicly accessible¹. The three datasets include optimization problems with architecture parameters \mathbf{x}_A only and a mixture of parameters with both \mathbf{x}_A and hyperparameters \mathbf{x}_H . We compare B²EA with nine benchmark algorithms. To ensure that our results are not misleading due to the choice of performance metric, we evaluate three different performance metrics. All our experimental results are based on **500** repetitions with random seeds, and the wall-clock times of both black-box function evaluation time and the NAS algorithm run-time are reflected. The details for reproducing our results can be found in Supplementary C.

Pre-evaluated NAS benchmark datasets: To facilitate scientific research on developing HPO and NAS algorithms, tabular benchmark datasets can be used [44, 20]. Our experiments are also based on these pre-evaluated and multi-fidelity benchmarks, and the NAS benchmarks we used are summarized in Table 1. The HPO-Bench [36] focuses on MLP regression problems with mixed variables $(\mathbf{x}_A, \mathbf{x}_H)$, and it was used as the main performance benchmark in Lee et al. [39]. The NAS-Bench includes NAS-Bench-101 [67] and NAS-Bench-201 [18], and they focus on the architecture variables \mathbf{x}_A . NAS-Bench-101 was used as the main performance benchmark in White et al. [64], Wang et al. [62] and as a benchmark in Letham et al. [40], Ru et al. [57]. Recently, NAS-Bench-201 was used as a benchmark in Zhang et al. [69], Chu et al. [11, 13], Hu et al. [32], Awad et al. [2]. DNN-Bench contains five CNN tasks and one RNN task with mixed variables $(\mathbf{x}_A, \mathbf{x}_H)$, and it was introduced and used in Cho et al. [9]. Together, the four benchmarks include 14 DNN optimization tasks with a wide range of task characteristics.

Benchmark algorithms: Random Search (RS) [5] is used as the baseline. GP [59], SMAC [33], and TPE [7] are BO algorithms known for their high performance for HPO. To emphasize that they are BO algorithms, we have referred to them as BO-GP, BO-SMAC, and BO-TPE in our work. BOHB [23] is a state-of-the-art multi-fidelity algorithm that combines hyperband [43] and TPE. HEBO is the winner of BBO challenge at NeurIPS2020, and it is known to perform very well for ML tasks [61]. DEEP-BO is a diversified BO method developed for DNN tasks [9]. BANANAS [64] is a BO-based algorithm for NAS tasks that utilizes meta-neural networks. Regularized Evolution Algorithm (REA) [55] is a state-of-the-art EA algorithm that discovered AmoebaNets.

Three performance metrics: To minimize the risk of biased interpretation of the experimental results, we evaluate three different performance metrics. The first is *intermediate regret* r_t at wall clock time t , which is a popular and commonly used metric in the HPO and NAS research community. The definition is $r_t = |f(\mathbf{x}^*) - f(\tilde{\mathbf{x}}_t)|$, where \mathbf{x}^* is the optimal configuration in \mathcal{X} , and $\tilde{\mathbf{x}}_t$ is the

¹The three datasets are the NAS benchmark datasets that were available at the time of our investigation.

best configuration found in time t . The optimal configuration \mathbf{x}^* should be known and used only for the purpose of evaluating r_t . The main disadvantage of r_t is that its value is dependent on the actual value of the loss metric, making the analysis and interpretation of r_t difficult because they are specific to each individual task. Note that the validation performance is used as a proxy for the true performance $f(\mathbf{x})$ for the pre-evaluated NAS benchmark datasets.

The second and third metrics are *success rate* $\mathbb{P}(\tau \leq t)$ and *expected time* $\mathbb{E}[\tau]$, which were adopted in Cho et al. [9]. Consider a random variable τ that represents the time required to achieve the target performance c . Then, $\mathbb{E}[\tau]$ is simply the expected time to achieve c , and it becomes a fixed-target metric. Now, if we choose a time budget t_b , then $\mathbb{P}(\tau \leq t_b)$ is the success rate of achieving performance c before t reaches t_b . Therefore, $\mathbb{P}(\tau \leq t_b)$ becomes a fixed-budget metric, which is also associated with a fixed target c . While the two metrics are intuitive and easily interpretable, they can be sensitive to the choices of c and t_b . To make the two metrics as neutral as possible, we determined c and t_b in a systematic and consistent manner over all 14 benchmarks. For c , we chose targets c_e, c_d and c_x in consideration of the difficulties for each pre-evaluated dataset, where c_e, c_d and c_x are chosen as the top 1 %, top 0.05 % and top 0.02 % performances of all configurations in the pre-evaluated dataset, respectively. For t_b of each dataset, we systematically chose it as the time for the best-performing algorithm to achieve a success rate of 99 %. Because c_e, c_d, c_x and t_b are chosen with a fixed method independent of the dataset, we believe that the expected time $\mathbb{E}[\tau]$ and the success rate $\mathbb{P}(\tau \leq t_b)$ serve as fair metrics.

Finally, there are cases where an algorithm fails to achieve c even after running for the maximum allowed run time t_{max} . In this case, it is obviously misleading to consider t_{max} as the time to achieve c . To address this issue, the expected time is adjusted to $\frac{\mathbb{P}(\tau \leq t_{max})\mathbb{E}_s[\tau] + (1 - \mathbb{P}(\tau \leq t_{max}))t_{max}}{\mathbb{P}(\tau \leq t_{max})}$ as in Auger & Hansen [1], where $\mathbb{E}_s[\tau]$ is the expected time of successful cases only.

Settings of B²EA: We use $K=M=10$, and mutation is applied with the probability of 0.5 for all of our experiments. This could have been extensively tuned for performance improvement, but we performed only a minimal amount of sanity checking with the goal of obtaining generalizable results. For diversified BO, we followed [9] and used {GP-EI, GP-PI, GP-UCB, RF-EI, RF-PI, RF-UCB} as individual BO models (i.e., $\{\hat{f}_1, \dots, \hat{f}_6\}$) with input warping and output power transformation in Turner et al. [61]. We also applied the early termination rule in Cho et al. [9] that is a very conservative multi-fidelity technique. For handling categorical variables, we used the adjacency matrix encoding of White et al. [65] for NAS-Bench and one-hot encoding for the rest.

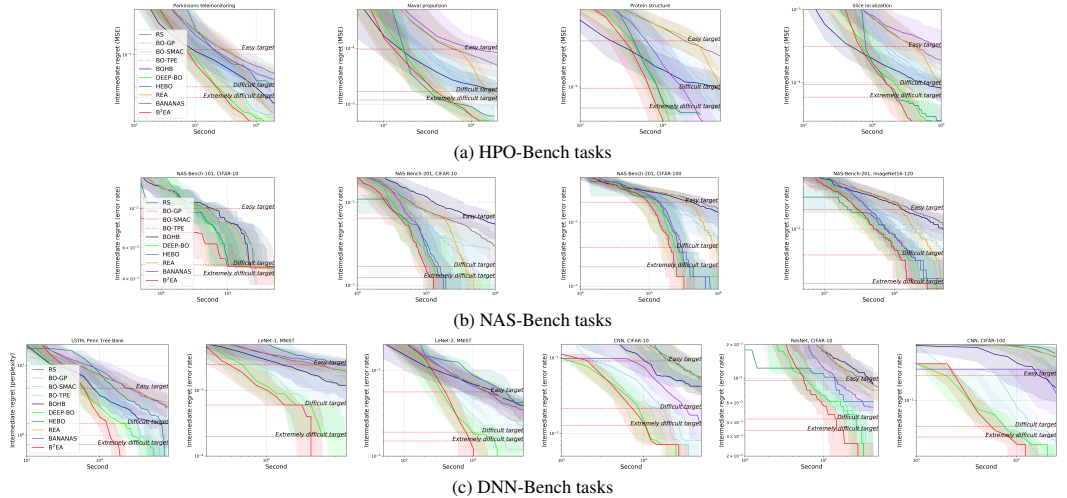


Figure 4: Performance in terms of intermediate regret metric r_t . The solid lines show the median r_t value of 500 runs, and the shaded areas show the interquartile range. The two axes are in logarithmic scales.

Experiment results: Figure 4 shows the intermediate regret r_t performance of the 500 runs. For success rate $\mathbb{P}(\tau \leq t)$ and expected time $\mathbb{E}[\tau]$, the results for the difficult target c_d are shown in Table 2 and Table 3, respectively. The full results including easy target c_e and extremely difficult

Table 2: Success rate $\mathbb{P}(\tau \leq t)$ performance (in %) for all benchmarks. The best performer in each task is shown in **bold**. The $\mathbb{P}(\tau \leq t)$ for c_e and c_x are presented in Table S1 of Supplementary A.

Target setting			Benchmark algorithms									Proposed algorithm
Goal	Source	Task name	RS	BO-GP	BO-SMAC	BO-TPE	BOHB	DEEP-BO	HEBO	BANANAS	REA	B ² EA
Difficult target c_d	HPO-Bench	Parkinsons	14.2	94.0	51.8	78.2	70.2	99.6	15.4	27.8	88.8	98.0
		Naval	4.4	38.4	24.0	47.4	32.6	97.4	99.4	3.6	13.8	98.6
		Protein	3.8	81.0	38.2	24.0	40.6	92.2	97.8	63.0	3.6	99.4
		Slice	5.8	31.6	39.2	39.2	52.8	84.6	99.6	5.4	23.4	90.4
	NAS-Bench-101	CIFAR-10	71.6	95.0	88.2	64.4	79.0	97.6	99.2	93.8	82.0	98.4
	NAS-Bench-201	CIFAR-10	7.4	74.4	16.0	47.8	3.4	78.4	96.6	86.0	67.8	99.2
		CIFAR-100	3.0	95.4	12.4	21.8	4.8	93.8	97.8	90.8	21.8	99.0
		ImageNet16-120	5.2	86.4	27.0	36.8	9.6	87.4	78.8	83.3	58.2	99.0
	DNN-Bench	PTB-LSTM	4.2	41.2	43.8	3.0	14.0	68.2	16.6	6.4	5.8	99.8
		MNIST-LeNet1	6.8	23.4	75.0	4.0	12.0	90.0	1.8	2.8	6.6	99.4
MNIST-LeNet2		7.0	21.2	65.4	5.0	0.0	77.2	3.0	6.2	7.4	99.0	
CIFAR10-CNN		5.0	85.2	82.2	8.4	0.0	96.0	6.4	50.8	9.2	99.2	
CIFAR10-ResNet		4.0	63.6	67.4	14.8	1.0	63.4	14.4	12.6	4.6	99.0	
CIFAR100-CNN		2.4	58.8	87.6	2.0	2.0	95.8	2.4	7.2	1.4	99.2	
Overall success rate	Mean	10.3	63.5	51.3	28.3	23.0	87.3	52.1	38.6	28.2	98.4	
	Std. deviation	0.2	0.3	0.3	0.2	0.3	0.1	0.5	0.4	0.3	0.0	
Overall rank	Mean	8.6	4.0	5.3	7.0	7.6	2.6	4.8	6.4	7.1	1.3	
	Std. deviation	1.5	1.1	2.2	1.8	2.1	0.9	3.3	2.2	1.7	0.5	

Table 3: Expected time $\mathbb{E}[\tau]$ performance (in *minutes*) for all benchmarks. The $\mathbb{E}[\tau]$ for c_e and c_x are presented in Table S2 of Supplementary A.

Target setting			Benchmark algorithms									Proposed algorithm
Goal	Source	Task name	RS	BO-GP	BO-SMAC	BO-TPE	BOHB	DEEP-BO	HEBO	BANANAS	REA	B ² EA
Difficult target c_d	HPO-Bench	Parkinsons	1,156.1	92.9	435.6	170.2	196.9	54.4	1,329.1	835.3	153.5	52.1
		Naval	1,450.9	298.0	711.3	242.5	385.9	67.0	54.9	5,840.2	330.4	67.2
		Protein	4,111.6	263.3	599.7	935.2	711.0	178.4	161.9	355.2	3,181.2	125.5
		Slice	9,549.0	3,511.4	2,491.4	2,068.3	1,705.7	661.3	326.5	24,380.9	2,152.8	472.7
	NAS-Bench-101	CIFAR-10	5,727	2,768	7,492	7,286	4,819	2,204	1,969	2,529	4,656	1,973
	NAS-Bench-201	CIFAR-10	58,474	6,153	74,382	11,031	128,338	5,108	3,147	3,700	6,492	1,986
		CIFAR-100	132,392	5,133	75,683	32,784	98,750	5,049	4,719	6,241	20,905	3,727
		ImageNet16-120	646,652	34,178	161,390	139,496	428,714	35,196	47,285	41,763	71,998	21,523
	DNN-Bench	PTB-LSTM	4,640	574	610	10,200	1,679	380	1,385	4,777	5,096	213
		MNIST-LeNet1	7,256	2,687	535	10,417	3,866	391	78,876	24,944	7,736	284
MNIST-LeNet2		3,917	1,333	387	6,833	8,566	294	12,799	5,129	2,313	134	
CIFAR10-CNN		5,248	318	307	4,576	84,194	187	6,832	636	7,739	195	
CIFAR10-ResNet		86,421	5,118	4,499	37,691	197,037	4,688	40,752	31,657	150,634	2,325	
CIFAR100-CNN		4,957	231	150	3,313	2,541	121	7,207	1,127	4,256	96	
Normalized $\mathbb{E}[\tau]$ (in %)	Mean	55.5	7.8	23.2	31.2	48.2	4.7	34.9	33.6	30.0	3.6	
	Std. deviation	33.1	9.1	29.5	31.9	37.4	7.3	43.4	33.7	28.0	6.6	

target c_x can be found in Supplementary A. From the three evaluation results, it can be observed that B²EA is the only method that shows a robust performance over all 14 benchmarks and all three difficulty levels. To understand the specialty of each algorithm, we have calculated the average $\mathbb{P}(\tau \leq t)$ performance over the three benches and the three difficulty levels. The results are shown in Table 4, and B²EA is the top ranker for all of the nine categories. DEEP-BO is the second ranker for HPO-Bench and DNN-Bench. HEBO is the second ranker for NAS-Bench. Considering that HEBO was not designed for NAS, this is an interesting result. Per-algorithm performance can be found in Table S2 of Supplementary A.

6 Discussion

Ablation studies: Ablation study results of B²EA’s enhancement techniques are shown in Table 5. When SAEA is turned off, the performance degrades over all nine cases. Therefore, we can observe that SAEA is a robust technique for the 14 benchmark tasks. Early termination is also a robust technique thanks to its conservative design, but its positive influence is also limited. On the contrary, HPO-Bench can benefit by having input warping turned off and NAS-Bench’s easy-target case can benefit by having output transformation turned off. The corresponding cases are shown in bold. Therefore, we can say that the two features are less robust over the 14 benchmarks. For the input warping, HPO-Bench’s tasks are less complicated than NAS-Bench’s or DNN-Bench’s tasks, and it can be speculated that input warping’s handling of non-stationary functions caused a negative effect instead of creating a positive effect. For the output transformation, it is unclear why it is helpful to

Table 4: Top-5 performers for each benchmark in terms of $\mathbb{P}(\tau \leq t)$ performance. They are ordered according to the ranking. Table for $\mathbb{E}[\tau]$ can be found in Table S3 of Supplementary A, and the top two rankers are exactly the same as in the below table.

Benchmark	Algorithm (Mean success rate $\mathbb{P}(\tau \leq t)$)		
	Easy target c_e	Difficult target c_d	Extremely difficult target c_x
HPO-Bench	B ² EA (98.4 %)	B ² EA (96.6 %)	B ² EA (97.7 %)
	DEEP-BO (94.8 %)	DEEP-BO (93.5 %)	DEEP-BO (92.3 %)
	HEBO (94.5 %)	HEBO (78.1 %)	HEBO (71.0 %)
	BOHB (92.3 %)	BO-GP (61.3 %)	BO-GP (54.9 %)
	BO-SMAC (81.7 %)	BOHB (49.1 %)	BO-TPE (39.3 %)
NAS-Bench	B ² EA (99.1 %)	B ² EA (98.9 %)	B ² EA (83.1 %)
	HEBO (95.5 %)	HEBO (93.1 %)	HEBO (71.8 %)
	BANANAS (93.3 %)	DEEP-BO (89.3 %)	BANANAS (68.1 %)
	BO-GP (89.8 %)	BANANAS (88.5 %)	DEEP-BO (59.4 %)
	DEEP-BO (89.3%)	BO-GP (87.8 %)	BO-GP (56.7 %)
DNN-Bench	B ² EA (99.1 %)	B ² EA (99.3 %)	B ² EA (98.4 %)
	DEEP-BO (95.5 %)	DEEP-BO (81.8 %)	DEEP-BO (70.4 %)
	BO-SMAC (82.8 %)	BO-SMAC (70.2 %)	BO-SMAC (62.6 %)
	BO-GP (66.4 %)	BO-GP (48.9 %)	BO-GP (37.5 %)
	BOHB (38.7 %)	BANANAS (14.3 %)	BANANAS (8.4 %)

Table 5: Ablation study results of B²EA: relative performance of $\mathbb{E}[\tau]$ with respect to B²EA is shown. Smaller values are better. For ‘SAEA off’, we have used GP-EI instead.

Enhancement techniques	HPO-Bench			NAS-Bench			DNN-Bench		
	c_e	c_d	c_x	c_e	c_d	c_x	c_e	c_d	c_x
B ² EA (everything on)	100.0	100.0	100.0	100.0	100.0	100.0	100.0	100.0	100.0
SAEA off	142.5	123.0	116.9	186.4	123.9	173.3	156.0	119.8	130.5
Input warping off	99.6	93.6	95.8	116.0	107.8	107.4	104.2	102.7	108.6
Output transformation off	148.3	299.7	455.1	96.8	179.2	227.6	129.9	227.7	306.6
Early termination off	101.6	101.7	102.0	104.3	107.1	103.2	124.3	117.4	112.6

have it off for the NAS-Bench’s easy-target case. In our experiments, generally output transformation turned out to be essential as can be seen from the three cases with extremely difficult target (c_x). For the extremely difficult target, the positive effect is understandable because NAS needs to be able to differentiate even a very small improvement in neural architecture performance when searching for an extremely well performing candidate. Ablation study results of SAEA’s three modules are shown in Table 6. We have listed only the meaningful combinations of on and off. It can be observed that all three modules are generally helpful. When the target performance is easy (c_e), however, removing mutation was helpful. This is in line with the common understanding of BO performing better than EA when the computation budget is small. This can be also confirmed in Figure 1 where REA’s performance is the worst for the extremely easy target.

Acquisition functions of BO: HEBO uses a multi-objective acquisition ensemble that aims to find Pareto-optimal points [14]. DEEP-BO simply uses a round-robin of BO models where EI, PI, and UCB take turns. When we compared the two approaches, both performed comparably (see Figure S3 of Supplementary D). Therefore, we have chosen to use simple round-robin or uniform random schemes in B²EA. As for the surrogate models, we can expect increasing diversity to be helpful and B²EA uses both GP and RF (see the results in Figure S4).

Modeling cost of BO models: Some of the BO models can have prohibitively high modeling costs when $|\mathcal{H}|$ is large. For instance, the complexity of GP is known to be $\mathcal{O}(|\mathcal{H}|^3)$. When the black-box optimization relies solely on the accuracy of a single BO model, evaluating all the samples in \mathcal{H} can be an essential goal. B²EA, however, utilizes a number of techniques including diversification, and it can be prudent to avoid such an expensive modeling or its work-arounds. Therefore, when $|\mathcal{H}|$ is larger than 200, we randomly sample only 200 samples from \mathcal{H} in each iteration and use them for GP modeling.

Table 6: Ablation study results of SAEA: relative performance of $\mathbb{E}[\tau]$ with respect to B²EA is shown. Smaller values are better. ‘DEEP-BO like’ can be regarded as a DEEP-BO improved with input warping and output transformation.

Module A/B/C	Standardized $\mathbb{E}[\tau]$			Remark
	c_e	c_d	c_x	
on/on/on	100.0	100.0	100.0	B ² EA
on/off/on	93.0	100.4	124.4	
off/off/on	101.5	103.4	125.9	DEEP-BO like
on/on/off	550.6	6423.3†	5138.3†	
on/off/off	472.8	2629.3	3618.1	
off/off/off	861.0	2764.7	4426.8	RS

† Failed experiments were excluded.

Modern neural architecture design: NAS algorithms have become an essential part of modern neural architecture design, and apparently there is a synergy effect over a variety of design methods including manual design, brute-force search, weight-sharing NAS, and multi-trial NAS. Once a neural architecture of high performance is published, a highly efficient NAS algorithm can be configured to optimize over a search space near the published neural architecture. The search space design will be dependent on the type of NAS. In fact, the success of recent NAS algorithms might be due to the highly constrained search space that was chosen based on the previously found high-performance architectures [46, 72, 45]. This is not necessarily a problem because NAS can benefit from any discovery of high-performance architectures through human effort, multi-trial NAS with a very large computational budget, or anything else.

7 Conclusions and Limitations

B²EA is a multi-trial NAS algorithm that is efficient because of the BO surrogate models and robust because of the diversification, cooperation, and mutation. Input warping, output transformation, and a conservative early termination turned out to be beneficial, too. We also note a few limitations of our work. We have performed experiments over 14 NAS tasks, but there are new benchmarks that have been published recently [37, 48, 41, 31]. We have adopted a conservative multi-fidelity technique, but less conservative multi-fidelity techniques are desired as long as robustness can be maintained. Parallelization is a fundamental technique for speeding up a search, and integrating parallelization techniques with B²EA remains as a future work.

8 Acknowledgements

This work was supported by an NRF grant (MSIT) under Grant NRF-2020R1A2C2007139, an ETRI grant [21ZR1100, A Study of Hyper-Connected Thinking Internet Technology by autonomous connecting, controlling and evolving ways], and an IITP grant (MSIT) [NO.2021-0-01343, Artificial Intelligence Graduate School Program (Seoul National University)].

References

- [1] Auger, A. and Hansen, N. Performance evaluation of an advanced local search evolutionary algorithm. In *2005 IEEE Congress on Evolutionary Computation*, volume 2, pp. 1777–1784 Vol. 2, 2005. doi: 10.1109/CEC.2005.1554903.
- [2] Awad, N., Mallik, N., and Hutter, F. Dehb: Evolutionary hyperband for scalable, robust and efficient hyperparameter optimization. *arXiv preprint arXiv:2105.09821*, 2021.
- [3] Baker, B., Gupta, O., Naik, N., and Raskar, R. Designing neural network architectures using reinforcement learning. *arXiv preprint arXiv:1611.02167*, 2016.
- [4] Bender, G., Kindermans, P.-J., Zoph, B., Vasudevan, V., and Le, Q. Understanding and simplifying one-shot architecture search. In *International Conference on Machine Learning*, pp. 550–559. PMLR, 2018.

- [5] Bergstra, J. and Bengio, Y. Random search for hyper-parameter optimization. *Journal of Machine Learning Research*, 13(Feb):281–305, 2012.
- [6] Bergstra, J., Yamins, D., and Cox, D. D. Making a science of model search: Hyperparameter optimization in hundreds of dimensions for vision architectures. *ICML (1)*, 28:115–123, 2013.
- [7] Bergstra, J. S., Bardenet, R., Bengio, Y., and Kégl, B. Algorithms for hyper-parameter optimization. In *Advances in neural information processing systems*, pp. 2546–2554, 2011.
- [8] Brock, A., Lim, T., Ritchie, J. M., and Weston, N. Smash: one-shot model architecture search through hypernetworks. *arXiv preprint arXiv:1708.05344*, 2017.
- [9] Cho, H., Kim, Y., Lee, E., Choi, D., Lee, Y., and Rhee, W. Basic enhancement strategies when using bayesian optimization for hyperparameter tuning of deep neural networks. *IEEE Access*, 8:52588–52608, 2020.
- [10] Choi, D., Cho, H., and Rhee, W. On the difficulty of dnn hyperparameter optimization using learning curve prediction. In *TENCON 2018-2018 IEEE Region 10 Conference*, pp. 0651–0656. IEEE, 2018.
- [11] Chu, X., Wang, X., Zhang, B., Lu, S., Wei, X., and Yan, J. Darts-: robustly stepping out of performance collapse without indicators. *arXiv preprint arXiv:2009.01027*, 2020.
- [12] Chu, X., Zhou, T., Zhang, B., and Li, J. Fair darts: Eliminating unfair advantages in differentiable architecture search. In *European Conference on Computer Vision*, pp. 465–480. Springer, 2020.
- [13] Chu, X., Zhang, B., and Xu, R. Fairnas: Rethinking evaluation fairness of weight sharing neural architecture search. In *Proceedings of the IEEE/CVF International Conference on Computer Vision*, pp. 12239–12248, 2021.
- [14] Cowen-Rivers, A. I., Lyu, W., Tutunov, R., Wang, Z., Grosnit, A., Rhys Griffiths, R., Maraval, A. M., Jianye, H., Wang, J., Peters, J., and Ammar, H. B. An Empirical Study of Assumptions in Bayesian Optimisation. *arXiv e-prints*, art. arXiv:2012.03826, December 2020.
- [15] Domhan, T., Springenberg, J. T., and Hutter, F. Speeding up automatic hyperparameter optimization of deep neural networks by extrapolation of learning curves. In *Proceedings of the 24th International Joint Conference on Artificial Intelligence (IJCAI)*, 2015.
- [16] Dong, X. and Yang, Y. One-shot neural architecture search via self-evaluated template network. In *Proceedings of the IEEE/CVF International Conference on Computer Vision*, pp. 3681–3690, 2019.
- [17] Dong, X. and Yang, Y. Searching for a robust neural architecture in four gpu hours. In *Proceedings of the IEEE Conference on computer vision and pattern recognition*, pp. 1761–1770, 2019.
- [18] Dong, X. and Yang, Y. Nas-bench-201: Extending the scope of reproducible neural architecture search. In *International Conference on Learning Representations (ICLR)*, 2020.
- [19] Dong, X., Liu, L., Musial, K., and Gabrys, B. Nats-bench: Benchmarking nas algorithms for architecture topology and size. *IEEE transactions on pattern analysis and machine intelligence*, 2021.
- [20] Eggenberger, K., Müller, P., Mallik, N., Feurer, M., Sass, R., Klein, A., Awad, N., Lindauer, M., and Hutter, F. Hpobench: A collection of reproducible multi-fidelity benchmark problems for hpo. *arXiv preprint arXiv:2109.06716*, 2021.
- [21] Elsken, T., Metzen, J. H., Hutter, F., et al. Neural architecture search: A survey. *J. Mach. Learn. Res.*, 20(55):1–21, 2019.
- [22] Emmerich, M. T., Giannakoglou, K. C., and Naujoks, B. Single-and multiobjective evolutionary optimization assisted by gaussian random field metamodells. *IEEE Transactions on Evolutionary Computation*, 10(4):421–439, 2006.

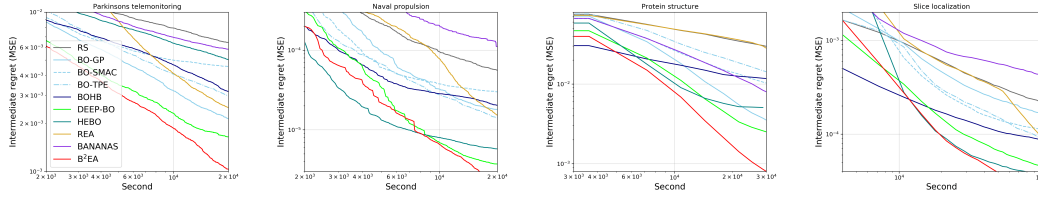
- [23] Falkner, S., Klein, A., and Hutter, F. BOHB: Robust and efficient hyperparameter optimization at scale. In Dy, J. and Krause, A. (eds.), *Proceedings of the 35th International Conference on Machine Learning*, volume 80 of *Proceedings of Machine Learning Research*, pp. 1437–1446. PMLR, 10–15 Jul 2018.
- [24] Golberg, D. E. Genetic algorithms in search, optimization, and machine learning. *Addison Wesley*, 1989(102):36, 1989.
- [25] Golovin, D., Solnik, B., Moitra, S., Kochanski, G., Karro, J., and Sculley, D. Google vizier: A service for black-box optimization. In *Proceedings of the 23rd ACM SIGKDD International Conference on Knowledge Discovery and Data Mining*, pp. 1487–1495. ACM, 2017.
- [26] González, J., Osborne, M., and Lawrence, N. Glasses: Relieving the myopia of bayesian optimisation. In *Artificial Intelligence and Statistics*, pp. 790–799. PMLR, 2016.
- [27] GPy. GPy: A gaussian process framework in python. <http://github.com/SheffieldML/GPy>, since 2012.
- [28] Guo, Z., Zhang, X., Mu, H., Heng, W., Liu, Z., Wei, Y., and Sun, J. Single path one-shot neural architecture search with uniform sampling. In *ECCV*, 2020.
- [29] Hansen, N., Auger, A., Ros, R., Mersmann, O., Tušar, T., and Brockhoff, D. Coco: A platform for comparing continuous optimizers in a black-box setting. *Optimization Methods and Software*, 36(1):114–144, 2021.
- [30] He, X., Zhao, K., and Chu, X. Automl: A survey of the state-of-the-art. *Knowledge-Based Systems*, 212:106622, 2021.
- [31] Hirose, Y., Yoshinari, N., and Shirakawa, S. Nas-hpo-bench-ii: A benchmark dataset on joint optimization of convolutional neural network architecture and training hyperparameters. In *Asian Conference on Machine Learning*, pp. 1349–1364. PMLR, 2021.
- [32] Hu, Y., Wang, X., Li, L., and Gu, Q. Improving one-shot nas with shrinking-and-expanding supernet. *Pattern Recognition*, 118:108025, 2021.
- [33] Hutter, F., Hoos, H. H., and Leyton-Brown, K. Sequential model-based optimization for general algorithm configuration. In *International Conference on Learning and Intelligent Optimization*, pp. 507–523. Springer, 2011.
- [34] Jaderberg, M., Dalibard, V., Osindero, S., Czarnecki, W. M., Donahue, J., Razavi, A., Vinyals, O., Green, T., Dunning, I., Simonyan, K., et al. Population based training of neural networks. *arXiv preprint arXiv:1711.09846*, 2017.
- [35] Jin, Y. Surrogate-assisted evolutionary computation: Recent advances and future challenges. *Swarm and Evolutionary Computation*, 1(2):61–70, 2011.
- [36] Klein, A. and Hutter, F. Tabular benchmarks for joint architecture and hyperparameter optimization. *arXiv preprint arXiv:1905.04970*, 2019.
- [37] Klyuchnikov, N., Trofimov, I., Artemova, E., Salnikov, M., Fedorov, M., and Burnaev, E. Nas-bench-nlp: neural architecture search benchmark for natural language processing. *arXiv preprint arXiv:2006.07116*, 2020.
- [38] Krizhevsky, A., Sutskever, I., and Hinton, G. E. Imagenet classification with deep convolutional neural networks. In *Proceedings of the 25th International Conference on Neural Information Processing Systems - Volume 1*, NIPS’12, pp. 1097–1105, Red Hook, NY, USA, 2012. Curran Associates Inc.
- [39] Lee, E., Eriksson, D., Bindel, D., Cheng, B., and Mccourt, M. Efficient rollout strategies for bayesian optimization. In *Conference on Uncertainty in Artificial Intelligence*, pp. 260–269. PMLR, 2020.
- [40] Letham, B., Calandra, R., Rai, A., and Bakshy, E. Re-examining linear embeddings for high-dimensional bayesian optimization. *Advances in Neural Information Processing Systems*, 33, 2020.

- [41] Li, C., Yu, Z., Fu, Y., Zhang, Y., Zhao, Y., You, H., Yu, Q., Wang, Y., and Lin, Y. Hw-nas-bench: Hardware-aware neural architecture search benchmark. *arXiv preprint arXiv:2103.10584*, 2021.
- [42] Li, L. and Talwalkar, A. Random search and reproducibility for neural architecture search. In *Uncertainty in Artificial Intelligence*, pp. 367–377. PMLR, 2020.
- [43] Li, L., Jamieson, K., DeSalvo, G., Rostamizadeh, A., and Talwalkar, A. Hyperband: A novel bandit-based approach to hyperparameter optimization. *The Journal of Machine Learning Research*, 18(1):6765–6816, 2017.
- [44] Lindauer, M. and Hutter, F. Best practices for scientific research on neural architecture search. *Journal of Machine Learning Research*, 21(243):1–18, 2020.
- [45] Liu, C., Zoph, B., Neumann, M., Shlens, J., Hua, W., Li, L.-J., Fei-Fei, L., Yuille, A., Huang, J., and Murphy, K. Progressive neural architecture search. In *Proceedings of the European conference on computer vision (ECCV)*, pp. 19–34, 2018.
- [46] Liu, H., Simonyan, K., Vinyals, O., Fernando, C., and Kavukcuoglu, K. Hierarchical representations for efficient architecture search. *arXiv preprint arXiv:1711.00436*, 2017.
- [47] Liu, H., Simonyan, K., and Yang, Y. Darts: Differentiable architecture search. *arXiv preprint arXiv:1806.09055*, 2018.
- [48] Mehrotra, A., Ramos, A. G. C., Bhattacharya, S., Dudziak, Ł., Yipperla, R., Chau, T., Abdelfattah, M. S., Ishtiaq, S., and Lane, N. D. Nas-bench-asr: Reproducible neural architecture search for speech recognition. In *International Conference on Learning Representations*, 2020.
- [49] Mlakar, M., Petelin, D., Tušar, T., and Filipič, B. Gp-demo: differential evolution for multi-objective optimization based on gaussian process models. *European Journal of Operational Research*, 243(2):347–361, 2015.
- [50] Mockus, J., Tiesis, V., and Zilinskas, A. chapter bayesian methods for seeking the extremum. *Toward global optimization, volume 2*, 1978.
- [51] Park, C., Borth, D. J., Wilson, N. S., Hunter, C. N., and Friedersdorf, F. J. Robust gaussian process regression with a bias model. *Pattern Recognition*, pp. 108444, 2021.
- [52] Pedregosa, F., Varoquaux, G., Gramfort, A., Michel, V., Thirion, B., Grisel, O., Blondel, M., Prettenhofer, P., Weiss, R., Dubourg, V., et al. Scikit-learn: Machine learning in python. *Journal of machine learning research*, 12(Oct):2825–2830, 2011.
- [53] Pham, H., Guan, M. Y., Zoph, B., Le, Q. V., and Dean, J. Efficient neural architecture search via parameter sharing. *arXiv preprint arXiv:1802.03268*, 2018.
- [54] Real, E., Moore, S., Selle, A., Saxena, S., Suematsu, Y. L., Le, Q., and Kurakin, A. Large-scale evolution of image classifiers. *arXiv preprint arXiv:1703.01041*, 2017.
- [55] Real, E., Aggarwal, A., Huang, Y., and Le, Q. V. Regularized evolution for image classifier architecture search. In *Proceedings of the aaai conference on artificial intelligence*, volume 33, pp. 4780–4789, 2019.
- [56] Rios, G. and Tobar, F. Compositionally-warped gaussian processes. *Neural Networks*, 118: 235–246, 2019.
- [57] Ru, B., Alvi, A., Nguyen, V., Osborne, M. A., and Roberts, S. Bayesian optimisation over multiple continuous and categorical inputs. In *International Conference on Machine Learning*, pp. 8276–8285. PMLR, 2020.
- [58] Shahriari, B., Swersky, K., Wang, Z., Adams, R. P., and De Freitas, N. Taking the human out of the loop: A review of bayesian optimization. *Proceedings of the IEEE*, 104(1):148–175, 2016.
- [59] Snoek, J., Larochelle, H., and Adams, R. P. Practical bayesian optimization of machine learning algorithms. In *Advances in neural information processing systems*, pp. 2951–2959, 2012.

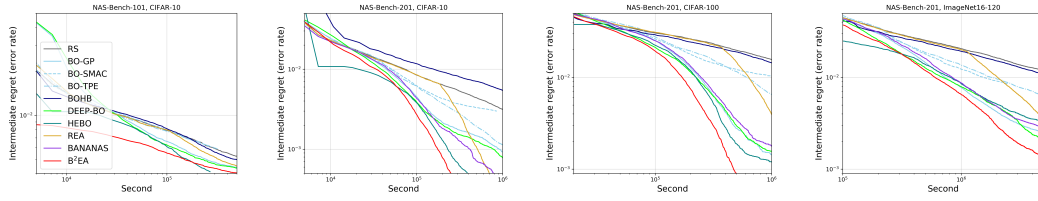
- [60] Snoek, J., Swersky, K., Zemel, R., and Adams, R. Input warping for bayesian optimization of non-stationary functions. In Xing, E. P. and Jebara, T. (eds.), *Proceedings of the 31st International Conference on Machine Learning*, Proceedings of Machine Learning Research, pp. 1674–1682, Beijing, China, 22–24 Jun 2014. PMLR.
- [61] Turner, R., Eriksson, D., McCourt, M. J., Kiili, J., Laaksonen, E., Xu, Z., and Guyon, I. Bayesian optimization is superior to random search for machine learning hyperparameter tuning: Analysis of the black-box optimization challenge 2020. In *NeurIPS*, 2020.
- [62] Wang, L., Zhao, Y., Jinnai, Y., Tian, Y., and Fonseca, R. Neural architecture search using deep neural networks and monte carlo tree search. *Proceedings of the AAAI Conference on Artificial Intelligence*, 34(06):9983–9991, Apr. 2020.
- [63] Wang, R., Cheng, M., Chen, X., Tang, X., and Hsieh, C.-J. Rethinking architecture selection in differentiable nas. In *International Conference on Learning Representations*, 2021.
- [64] White, C., Neiswanger, W., and Savani, Y. Bananas: Bayesian optimization with neural architectures for neural architecture search. *arXiv preprint arXiv:1910.11858*, 2019.
- [65] White, C., Neiswanger, W., Nolen, S., and Savani, Y. A study on encodings for neural architecture search. *arXiv preprint arXiv:2007.04965*, 2020.
- [66] Yan, S., White, C., Savani, Y., and Hutter, F. Nas-bench-x11 and the power of learning curves. *Advances in Neural Information Processing Systems*, 34, 2021.
- [67] Ying, C., Klein, A., Christiansen, E., Real, E., Murphy, K., and Hutter, F. Nas-bench-101: Towards reproducible neural architecture search. In *International Conference on Machine Learning*, pp. 7105–7114. PMLR, 2019.
- [68] Zela, A., Elsken, T., Saikia, T., Marrakchi, Y., Brox, T., and Hutter, F. Understanding and robustifying differentiable architecture search. *arXiv preprint arXiv:1909.09656*, 2019.
- [69] Zhang, M., Li, H., Pan, S., Chang, X., Zhou, C., Ge, Z., and Su, S. W. One-shot neural architecture search: Maximising diversity to overcome catastrophic forgetting. *IEEE Transactions on Pattern Analysis and Machine Intelligence*, 2020.
- [70] Zhu, H., An, Z., Yang, C., Xu, K., Zhao, E., and Xu, Y. Eena: efficient evolution of neural architecture. In *Proceedings of the IEEE/CVF International Conference on Computer Vision Workshops*, pp. 0–0, 2019.
- [71] Zoph, B. and Le, Q. V. Neural architecture search with reinforcement learning. *arXiv preprint arXiv:1611.01578*, 2016.
- [72] Zoph, B., Vasudevan, V., Shlens, J., and Le, Q. V. Learning transferable architectures for scalable image recognition. In *Proceedings of the IEEE conference on computer vision and pattern recognition*, pp. 8697–8710, 2018.

Supplementary materials

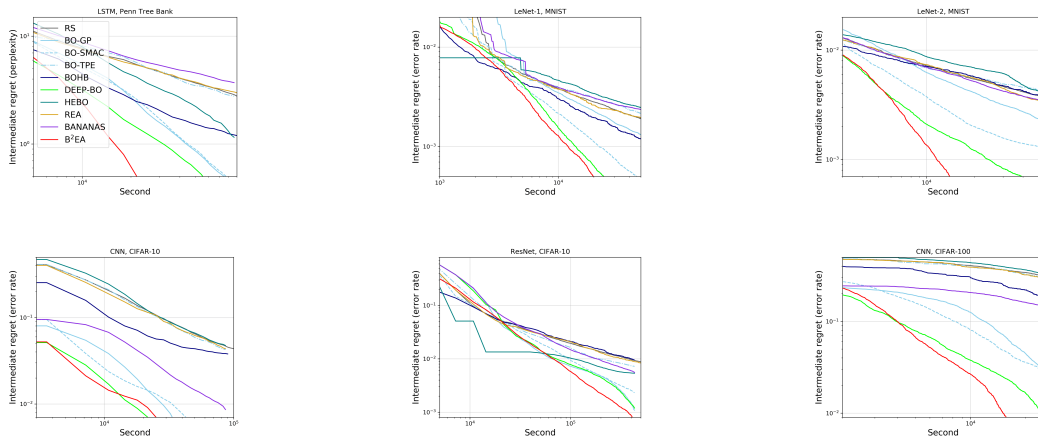
A Full Benchmark Results



(a) HPO-Bench tasks.



(b) NAS-Bench tasks.



(c) DNN-Bench tasks.

Figure S1. Comparison of intermediate regret r_t performance, but plotted for *mean* r_t value of 500 repeated runs.

Table S1. Success rate $\mathbb{P}(\tau \leq t)$ performance (in %) for all benchmarks. We measured $\mathbb{P}(\tau \leq t)$ at time t when the best-performing algorithm achieved a success rate of 99%. The best performer in each task is shown in **bold**.

Target setting			Benchmark algorithms									Proposed algorithm
Goal	Source	Task name	RS	BO-GP	BO-SMAC	BO-TPE	BOHB	DEEP-BO	HEBO	BANANAS	REA	B ² EA
Easy target c_e	HPO-Bench	Parkinsons	71.8	95.8	96.0	91.8	97.8	99.0	80.8	78.2	74.6	99.4
		Naval	35.6	65.8	76.8	76.0	84.2	95.0	99.0	29.0	29.2	97.0
		Protein	34.6	81.2	79.8	65.2	94.8	93.8	99.2	78.0	30.6	98.6
		Slice	30.0	61.2	74.2	68.2	92.2	91.2	99.0	27.2	32.6	98.6
	NAS-Bench-101	CIFAR-10	55.6	74.6	56.4	63.0	49.0	76.0	86.0	88.4	65.0	99.4
	NAS-Bench-201	CIFAR-10	56.6	95.8	85.0	90.8	33.2	96.8	99.6	95.2	78.0	98.8
		CIFAR-100	39.6	92.8	78.8	74.4	48.6	92.0	98.0	93.4	48.2	99.0
		ImageNet16-120	36.0	95.8	81.0	75.2	43.2	92.4	98.4	96.0	37.8	99.0
	DNN-Bench	PTB-LSTM	31.8	63.2	68.6	26.0	80.0	92.0	44.4	36.0	27.0	99.0
		MNIST-LeNet1	35.8	56.4	83.6	24.0	63.0	96.8	23.0	30.6	44.0	99.2
		MNIST-LeNet2	35.8	56.8	87.6	39.0	29.0	96.8	17.0	38.6	36.0	99.2
		CIFAR10-CNN	13.2	74.6	87.8	16.0	21.0	99.2	4.0	15.8	13.6	99.6
CIFAR10-ResNet		22.8	95.4	87.6	32.0	13.0	89.2	44.6	45.6	22.8	99.0	
CIFAR100-CNN		8.0	52.2	81.8	9.0	26.0	99.0	4.0	14.4	6.8	98.6	
Overall success rate	Mean	36.2	75.8	80.4	53.6	55.4	93.5	64.1	54.7	39.0	98.9	
	Std. deviation	16.7	16.8	9.6	28.3	29.7	6.0	31.9	31.5	21.3	0.6	
Overall rank	Mean	8.7	4.6	4.8	6.9	6.1	3.0	5.0	6.2	8.2	1.4	
	Std. deviation	0.9	1.3	1.6	1.3	2.9	1.2	3.8	2.5	1.2	0.5	
Difficult target c_d	HPO-Bench	Parkinsons	14.2	94.0	51.8	78.2	70.2	99.6	15.4	27.8	88.8	98.0
		Naval	4.4	38.4	24.0	47.4	32.6	97.4	99.4	3.6	13.8	98.6
		Protein	3.8	81.0	38.2	24.0	40.6	92.2	97.8	63.0	3.6	99.4
		Slice	5.8	31.6	39.2	39.2	52.8	84.6	99.6	5.4	23.4	90.4
	NAS-Bench-101	CIFAR-10	71.6	95.0	88.2	64.4	79.0	97.6	99.2	93.8	82.0	98.4
	NAS-Bench-201	CIFAR-10	7.4	74.4	16.0	47.8	3.4	78.4	96.6	86.0	67.8	99.2
		CIFAR-100	3.0	95.4	12.4	21.8	4.8	93.8	97.8	90.8	21.8	99.0
		ImageNet16-120	5.2	86.4	27.0	36.8	9.6	87.4	78.8	83.3	58.2	99.0
	DNN-Bench	PTB-LSTM	4.2	41.2	43.8	3.0	14.0	68.2	16.6	6.4	5.8	99.8
		MNIST-LeNet1	6.8	23.4	75.0	4.0	12.0	90.0	1.8	2.8	6.6	99.4
		MNIST-LeNet2	7.0	21.2	65.4	5.0	0.0	77.2	3.0	6.2	7.4	99.0
		CIFAR10-CNN	5.0	85.2	82.2	8.4	0.0	96.0	6.4	50.8	9.2	99.2
CIFAR10-ResNet		4.0	63.6	67.4	14.8	1.0	63.4	14.4	12.6	4.6	99.0	
CIFAR100-CNN		2.4	58.8	87.6	2.0	2.0	95.8	2.4	7.2	1.4	99.2	
Overall success rate	Mean	10.3	63.5	51.3	28.3	23.0	87.3	52.1	38.6	28.2	98.4	
	Std. deviation	17.9	27.6	26.5	24.5	27.4	11.5	45.7	37.5	31.6	2.3	
Overall rank	Mean	8.6	4.0	5.3	7.0	7.6	2.6	4.8	6.4	7.1	1.3	
	Std. deviation	1.5	1.1	2.2	1.8	2.1	0.9	3.3	2.2	1.7	0.5	
Extremely difficult target c_x	HPO-Bench	Parkinsons†	9.2	89.6	30.8	67.0	58.4	96.8	14.0	17.6	82.4	98.8
		Naval	3.2	28.6	14.4	42.0	20.4	98.2	96.6	1.6	22.6	99.0
		Protein	1.8	82.8	33.0	15.8	23.6	91.4	78.0	62.0	3.0	98.4
		Slice†	4.8	18.4	20.2	32.4	33.8	82.6	95.4	2.2	28.4	94.4
	NAS-Bench-101	CIFAR-10†	7.0	24.4	78.2	11.4	6.4	27.0	72.8	84.2	25.0	41.0
	NAS-Bench-201	CIFAR-10	8.4	75.4	16.2	51.8	3.6	79.6	97.2	76.8	76.2	99.2
		CIFAR-100	1.6	66.4	5.0	16.6	2.2	64.0	68.2	76.8	17.2	99.0
		ImageNet16-120†	3.2	60.6	17.2	24.0	5.8	67.0	48.8	34.4	45.2	93.0
	DNN-Bench	PTB-LSTM	2.0	34.2	31.8	0.0	9.0	40.2	14.8	2.6	3.4	99.2
		MNIST-LeNet1†	3.4	15.6	62.8	1.0	4.0	70.8	0.0	1.2	5.2	94.8
		MNIST-LeNet2	5.6	14.2	62.4	4.0	0.0	69.8	3.0	4.8	7.0	99.0
		CIFAR10-CNN	3.0	86.4	76.6	1.2	0.0	97.2	0.4	28.6	5.6	99.0
CIFAR10-ResNet		2.4	47.4	58.0	7.2	1.0	56.6	3.2	9.0	2.6	99.0	
CIFAR100-CNN		0.4	27.0	83.8	1.0	3.0	87.8	1.0	4.2	0.6	99.2	
Overall success rate	Mean	4.0	47.9	42.2	19.7	12.2	73.5	42.4	29.0	23.2	93.8	
	Std. deviation	2.7	28.1	27.1	21.3	16.7	21.6	40.7	32.1	27.0	15.3	
Overall rank	Mean	8.6	4.0	5.3	7.0	7.6	2.6	4.8	6.4	7.1	1.3	
	Std. deviation	1.5	1.1	2.2	1.8	2.1	0.9	3.3	2.2	1.7	0.5	

† Target performance could not be achieved even after using the maximum budget. Therefore, performance was measured for the maximum budget (i.e. $t_x = t_{max}$).

Table S2. Expected time $\mathbb{E}[\tau]$ performance (in minutes) for all benchmarks. The best performer in each task is shown in **bold**.

Target setting			Benchmark algorithms									Proposed algorithm	
Goal	Source	Task name	RS	BO-GP	BO-SMAC	BO-TPE	BOHB	DEEP-BO	HEBO	BANANAS	REA	B ² EA	
Easy target c_e	HPO-Bench	Parkinsons	68.7	25.4	26.0	33.3	19.7	15.9	47.5	61.7	54.7	14.6	
		Naval	149.1	54.1	54.6	49.8	34.6	26.7	23.5	276.1	108.7	22.8	
		Protein	418.6	123.1	134.9	189.9	61.0	86.0	75.2	151.6	369.5	64.2	
		Slice	944.2	434.4	302.1	331.1	124.7	170.9	134.4	1,970.4	630.6	115.5	
	NAS-Bench-101	CIFAR-10	1,062	714	1,362	1,088	1,214	678	460	439	893	101	
		CIFAR-100	4,391	1,206	2,238	1,727	13,407	1,010	919	1,264	2,570	848	
	NAS-Bench-201	CIFAR-100	12,220	2,739	4,898	4,900	10,012	2,648	2,479	2,751	6,288	1,842	
		ImageNet16-120	37,946	7,066	11,313	13,526	32,713	6,674	4,529	7,646	18,680	5,349	
	DNN-Bench	PTB-LSTM	586	191	183	535	142	109	362	644	607	102	
		MNIST-LeNet1	594	348	158	757	259	104	1,219	1,114	664	79	
		MNIST-LeNet2	378	215	100	469	392	60	557	331	353	66	
		CIFAR10-CNN	506	56	50	453	213	28	480	135	456	31	
		CIFAR10-ResNet	7,118	1,040	1,212	6,496	10,244	1,082	2,351	3,370	6,572	887	
		CIFAR100-CNN	880	119	82	727	367	32	1,205	445	889	40	
Normalized $\mathbb{E}[\tau]$ (in %)	Mean	75.9	24.2	27.1	52.9	50.4	15.3	46.4	54.1	61.8	10.4		
Std. deviation	23.4	12.7	23.5	26.1	35.5	11.8	38.8	34.4	22.5	5.2			
Difficult target c_d	HPO-Bench	Parkinsons	1,156.1	92.9	435.6	170.2	196.9	54.4	1,329.1	835.3	153.5	52.1	
		Naval	1,450.9	298.0	711.3	242.5	385.9	67.0	54.9	5,840.2	330.4	67.2	
		Protein	4,111.6	263.3	599.7	935.2	711.0	178.4	161.9	355.2	3,181.2	125.5	
		Slice	9,549.0	3,511.4	2,491.4	2,068.3	1,705.7	661.3	326.5	24,380.9	2,152.8	472.7	
	NAS-Bench-101	CIFAR-10	5,727	2,768	7,492	7,286	4,819	2,204	1,969	2,529	4,656	1,973	
		CIFAR-100	58,474	6,153	74,382	11,031	128,338	5,108	3,147	3,700	6,492	1,986	
	NAS-Bench-201	CIFAR-100	132,392	5,133	75,683	32,784	98,750	5,049	4,719	6,241	20,905	3,727	
		ImageNet16-120	646,652	34,178	161,390	139,496	428,714	35,196	47,285	41,763	71,998	21,523	
	DNN-Bench	PTB-LSTM	4,640	574	610	10,200	1,679	380	1,385	4,777	5,096	213	
		MNIST-LeNet1	7,256	2,687	535	10,417	3,866	391	78,876	24,944	7,736	284	
		MNIST-LeNet2	3,917	1,333	387	6,833	8,566	294	12,799	5,129	2,313	134	
		CIFAR10-CNN	5,248	318	307	4,576	84,194	187	6,832	636	7,739	195	
		CIFAR10-ResNet	86,421	5,118	4,499	37,691	197,037	4,688	40,752	31,657	150,634	2,325	
		CIFAR100-CNN	4,957	231	150	3,313	2,541	121	7,207	1,127	4,256	96	
Normalized $\mathbb{E}[\tau]$ (in %)	Mean	55.5	7.8	23.2	31.2	48.2	4.7	34.9	33.6	30.0	3.6		
Std. deviation	33.1	9.1	29.5	31.9	37.4	7.3	43.4	33.7	28.0	6.6			
Extremely difficult target c_x	HPO-Bench	Parkinsons	2,049	150	1,049	294	316	94	2,456	1,834	218	78	
		Naval	3,222	588	1,464	401	722	88	82	14,839	522	88	
		Protein	7,677	306	914	1,808	1,247	217	315	487	6,077	160	
		Slice	18,538	7,829	5,947	3,323	3,353	849	524	74,631	3,253	551	
	NAS-Bench-101	CIFAR-10	66,742	28,286	114,334	52,367	78,461	20,009	7,402	4,170	26,365	15,089	
		CIFAR-100	138,779	8,824	184,487	21,380	267,942	7,340	5,527	6,857	8,500	2,452	
	NAS-Bench-201	CIFAR-100	255,135	7,844	185,194	45,525	174,796	8,215	7,474	9,259	26,393	4,148	
		ImageNet16-120	1,427,033	76,921	294,908	275,107	785,983	74,433	118,953	162,487	116,940	37,488	
	DNN-Bench	PTB-LSTM	8,756	772	883	∞	3,262	676	1,623	9,975	7,732	263	
		MNIST-LeNet1	14,743	4,505	793	47,326	9,089	643	∞	59,236	9,300	458	
		MNIST-LeNet2	6,991	2,665	702	9,924	18,524	529	24,555	12,159	10,969	186	
		CIFAR10-CNN	9,684	373	392	19,031	∞	224	42,028	1,175	12,440	233	
		CIFAR10-ResNet	140,961	7,203	5,811	66,749	197,037	5,652	212,288	49,325	233,875	2,431	
		CIFAR100-CNN	15,568	368	209	14,047	4,950	196	17,548	2,030	11,557	139	
Normalized $\mathbb{E}[\tau]$ (in %)	Mean	61.0	6.7	25.2	31.4	43.6	3.7	40.9	41.9	33.9	2.3		
Std. deviation	32.0	6.0	32.6	25.9	33.0	4.4	47.3	43.1	33.4	3.3			

Table S3. Top-5 performers for each benchmark in terms of normalized expected time $\mathbb{E}[\tau]$ performance. They are ordered according to the ranking.

Benchmark	Algorithm (Normalized mean $\mathbb{E}[\tau]$)		
	Easy target c_e	Difficult target c_d	Extremely difficult target c_x
HPO-Bench	B ² EA (12.67)	B ² EA (2.52)	B ² EA (1.65)
	DEEP-BO (15.51)	DEEP-BO (3.07)	DEEP-BO (2.09)
	BOHB (15.54)	BO-GP (8.23)	BO-GP (6.13)
	HEBO (25.62)	BOHB (11.43)	BO-TPE (10.67)
	BO-SMAC (26.31)	HEBO (26.55)	HEBO (26.34)
NAS-Bench	B ² EA (10.73)	B ² EA (8.51)	B ² EA (1.65)
	HEBO (18.20)	HEBO (9.90)	HEBO (4.95)
	BANANAS (21.08)	DEEP-BO (10.66)	BANANAS (5.31)
	DEEP-BO (24.15)	BANANAS (11.95)	DEEP-BO (7.17)
	BO-GP (25.61)	BO-GP (12.73)	BO-GP (9.12)
DNN-Bench	B ² EA (8.72)	B ² EA (1.04)	B ² EA (1.09)
	DEEP-BO (9.14)	DEEP-BO (1.80)	DEEP-BO (2.35)
	BO-SMAC (14.64)	BO-SMAC (2.40)	BO-SMAC (2.94)
	BO-GP (21.32)	BO-GP (4.27)	BO-GP (5.38)
	BOHB (47.75)	BANANAS (25.17)	BANANAS (47.50)

Table S4. Summary of normalized expected time $\mathbb{E}[\tau]$ performance for each benchmark. Performance worse than random search is shown in red color.

Target	Benchmark	RS	BO-GP	BO-SMAC	BO-TPE	BOHB	DEEP-BO	HEBO	BANANAS	REA	B ² EA
Easy target c_e	HPO-Bench	75.5	27.0	26.3	32.2	15.5	15.5	25.6	81.5	59.8	12.7
	NAS-Bench	77.7	25.6	46.6	42.1	89.3	24.1	18.2	21.1	46.3	10.7
	DNN-Bench	75.0	21.3	14.6	73.8	47.7	9.1	79.0	57.9	73.4	8.7
Difficult target c_d	HPO-Bench	62.75	8.23	17.44	12.05	11.43	3.07	26.55	67.87	25.85	2.52
	NAS-Bench	80.50	12.73	60.02	38.05	76.30	10.66	9.90	11.95	23.53	8.51
	DNN-Bench	34.03	4.27	2.40	39.52	53.92	1.80	57.06	25.17	37.09	1.04
Extremely difficult target c_x	HPO-Bench	57.50	6.13	18.11	10.67	9.62	2.09	26.34	70.25	23.97	1.65
	NAS-Bench	77.54	9.12	65.53	22.73	73.05	7.17	4.95	5.31	11.19	4.59
	DNN-Bench [†]	52.19	5.38	2.94	Fail	Fail	2.35	Fail	47.50	55.56	1.09

[†] Compared with the algorithms that achieve the target at least once.

Algorithm S1. B²EA

Inputs: black-box function f , diversified BO models $\{\hat{f}_1, \dots, \hat{f}_B\}$, full search space \mathcal{X}

— Initialization
Choose $\mathbf{x}_1^{init}, \mathbf{x}_2^{init} \in \mathcal{X}$
Evaluate $\mathbf{y}_1^{init} \leftarrow f(\mathbf{x}_1^{init}), \mathbf{y}_2^{init} \leftarrow f(\mathbf{x}_2^{init})$
Set $\mathcal{H} \leftarrow \{(\mathbf{x}_1^{init}, \mathbf{y}_1^{init}), (\mathbf{x}_2^{init}, \mathbf{y}_2^{init})\}$

for $n = 1, 2, \dots$ **do**

— Module A (Populate with first BO)
 Set \hat{f}_{1st} as \hat{f}_m where $m = \text{mod}(n, B) + 1$
 Set \mathcal{P}^n as $\arg \text{top-k}_{\mathbf{x} \in \mathcal{X}} \hat{f}_{1st}(\mathbf{x}; \mathcal{H})$

— Module B (Apply genetic operator)
 Start with K parents. Apply mutation with the probability of 0.5 to form \mathcal{C}^n that contains M offspring.

— Module C (1. Estimate and choose the best with second BO; 2. Evaluate)
 Set \hat{f}_{2nd} as one of $\{\hat{f}_1, \dots, \hat{f}_B\}$. Choose randomly but exclude \hat{f}_{1st} ($= \hat{f}_m$).
 Select $\mathbf{x}^n \in \arg \max_{\mathbf{x} \in \mathcal{C}^n} \hat{f}_{2nd}(\mathbf{x}; \mathcal{H})$
 Evaluate $y_n \leftarrow f(\mathbf{x}_n)$

— Stop Criteria
 Check for exit criteria

— Update \mathcal{H}
 Update $\mathcal{H} \leftarrow \mathcal{H} \cup \{(\mathbf{x}_n, y_n)\}$

end for

***Note:** For simplicity, we omitted $k(\cdot)$ and $g(\cdot)$ for surrogate \hat{f} modeling, and also early termination strategy $f_{et}(\cdot)$.

B Implementation Details

First, we note that the code is provided as a part of the supplementary material. To produce the experiment results in our work, the proposed algorithms and the benchmark algorithms were merged into a unified package. Because the software licenses included in this project are all GPL-compatible, the code will be open-sourced under the GPL-3.0 license.

Proposed algorithms are designed to be a meta-heuristic algorithm framework where the Evolutionary Algorithm (EA) and Bayesian Optimization (BO) can harmonize in a unified manner. In this regard, we implemented the following components:

- **EA components:** While we followed the workflow similar to the implementation² of Real et al. [55], the mutation for the mixed-type parameters was newly implemented.
- **BO models:** To utilize two different models and three acquisition functions, we started from publicly available codes and partially implemented the Gaussian process (GP) model, random forest (RF) model, and the associated utility functions. The GP model was based on the `InputWarpedGP` class of the GPy library [27] and our RF model was based on the `RandomForestRegressor` class of the scikit-learn library [52], which is open-sourced under a BSD license. More specifically, the kernel design in our GP model is almost the same as HEBO [14], where the linear and Mat’ern 3/2 kernels were used with automatic relevance determination. However, its hyper-parameters were solely sampled using Monte Carlo estimation of the acquisition function values to reduce the modeling cost of GP regression. Second, the number of trees in our RF model has been set to 50, and the minimum number of elements in a split has been set at two. For the three acquisition functions, Snoek’s implementation³ was used with the noise *epsilon* set to 0.0001.
- **Input transformation:** For our input warped GP model, the cumulative distribution function of the Kumaraswamy distribution was used to handle non-stationary functions [60].
- **Output transformation:** To stabilize variance and minimize skewness in the power transformation, the box-cox and yeo-johnson transformations were employed in the same way as

²https://colab.research.google.com/github/google-research/google-research/blob/master/evolution/regularized_evolution_algorithm/regularized_evolution.ipynb

³github.com/JasperSnoek/sparmint/tree/master/sparmint

in HEBO [14]. For each transformation, the `power_transform` implementation from the `scikit-learn` was used.

- **Early termination rule:** We adopted the basic heuristics of Cho et al. [9] for the early termination based on DEEP-BO⁴, released under a GPL-3.0 license. Based on the prior assumption of the correlation between validation performance during training and the best one found after completion, the early termination rule percentile β controls the proper value of thresholds in earlier and later training epochs. Similar to Cho et al. [9], β was set to 0.1 for joint HPO-NAS tasks (HPO-Bench and DNN-Bench). Because the NAS-Bench tasks have been carefully tuned for training-related parameters, β was set to 0.25 for NAS-Bench tasks.

Benchmark algorithms are officially implemented in the following packages with the associated software license: *SpearMint* [59] (GPL-3), *Hyperopt* [6] (proprietary), *HpBandSter* [23] (BSD-3), *naszilla* [64] (Apache-2.0), and *HEBO* [14] (MIT). Specifically, the following references were used in our benchmark experiments:

- AutoML NAS experiments⁵ (BSD-3)
- NAS201 experiments⁶ (MIT)
- BANANAS experiments⁷ (Apache-2.0)

⁴github.com/snu-ads1/DEEP-BO

⁵https://github.com/automl/nas_benchmarks/tree/development/experiment_scripts

⁶<https://github.com/D-X-Y/AutoDL-Projects/blob/master/docs/NAS-Bench-201.md>

⁷<https://github.com/naszilla/naszilla>

C Experimental Details

Table S5. Summary of target and budget settings. To fairly compare the overall benchmark tasks, two target goals c_e , c_d and, c_x were set as the top 1 %, 0.05 % and 0.02 % best configuration performances, respectively. In addition, the values of t_e , t_d and t_x were determined when any algorithm was over 99 % for $\mathbb{P}(\tau \leq t)$ according to the target performance setting. If no algorithm could successfully achieve the above condition, the time was set to be the same as the maximum budget.

Source	Task	Easy target		Difficult target		Extremely difficult target		Max budget t_{max}
		Regret c_e	Budget t_e	Regret c_d	Budget t_d	Regret c_x	Budget t_x	
HPO-Bench	Parkinsons†	0.0114	80m	0.00459	240m	0.00353	300m	300m
	Naval	9.74109E-05	90m	1.71E-05	180m	1.19E-05	252m	300m
	Protein	0.034537211	190m	0.00957	360m	0.00568	480m	500m
	Slice†	0.000312	6h	9.46E-05	21h	9.35E-05	28h	28h
NAS-101-Bench	CIFAR-10†	0.01	16h	0.0048	130h	0.0041	138h	138h
NAS-201-Bench	CIFAR-10	0.00648	65h	0.00168	120h	0.00168	132h	138h
	CIFAR-100	0.0206	108h	0.004	192h	0.002	205h	277h
	ImageNet16-120†	0.017	294h	0.005	1124h	0.002	1388h	1388h
DNN-Bench	PTB-LSTM	4.7	5h	1.456	8h	0.734	9h	12h
	MNIST-LeNet1†	0.0025	280m	0.0006	12h	0.0002	12h	12h
	MNIST-LeNet2	0.0056	3h	0.0019	7h	0.0015	12h	15h
	CIFAR10-CNN	0.0908	80m	0.0213	9h	0.0128	10h	14h
	CIFAR10-ResNet	0.0155	45h	0.0055	108h	0.0034	108h	120h
	CIFAR100-CNN	0.2059	110m	0.0471	4h	0.03477	5h	7h

m and *h* refer to minute and hour, respectively.

† No algorithm could achieve over 99 % of success rate for t_x until the maximum budget t_{max} was used.

Tabular benchmark datasets: As summarized in the experiment section of the paper, we used four benchmark datasets saved as database files. Specifically in NAS-Bench, we used the files as following: *nasbench_full.tfrecord* and *NAS-Bench-201-v1_1-096897.pth*.

Computing environment: In general, the training time of a DNN is highly dependent on the specific hardware and the version of DL library. In our experiments, however, the training time was consistently calculated thanks to the use of tabular benchmark datasets. We randomized the computing resource assignments among different computing machines to measure the modeling time of surrogate functions. Intel Core i7 processors are commonly employed in our local devices. C5 instances are utilized in Amazon EC2. The modeling time is significantly less than DNN training time anyway.

Invalid candidate handling: Even when we tested all the algorithms on a well-defined search space, some candidate configurations could not provide satisfactory results due to known limitations. For instance, a performance record of a valid configuration can be absent in the lookup table because of the constraints on the data generation process in NAS-Bench-101. In this regard, we considered the following fail-over: if the specification of a candidate was invalid, then we removed this case from the candidate set or chose a valid one instead. Moreover, if a candidate was valid but its result was not in the database, then we approximated it to the one whose evaluation result existed in the table.

D Further Explanations

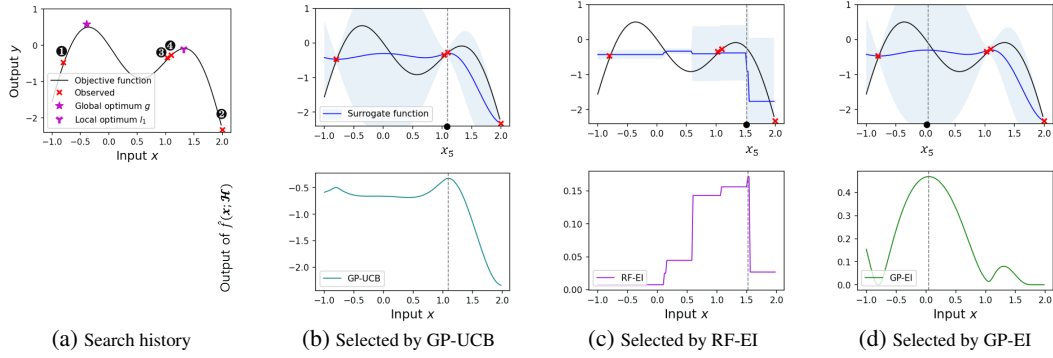


Figure S2. Catastrophic behavior of a single BO and diversification as a remedy. An optimization problem with one dimensional search space is shown in (a) where four candidates have been evaluated so far. In (b), GP-UCB selects the next candidate x_5 very close to the previously tried candidates x_3 and x_4 , and subsequently becomes stuck near them. In (c), the situation is better but RF-EI also selects a point near the local optimum l_1 . In (d), GP-EI has a different inductive bias and selects the next candidate near the global optimum g . In general, it is impossible to tell which model will avoid a catastrophic behavior, but ensemble of multiple acquisition functions [14] or rotating over multiple BOs [9] is known to be robust.

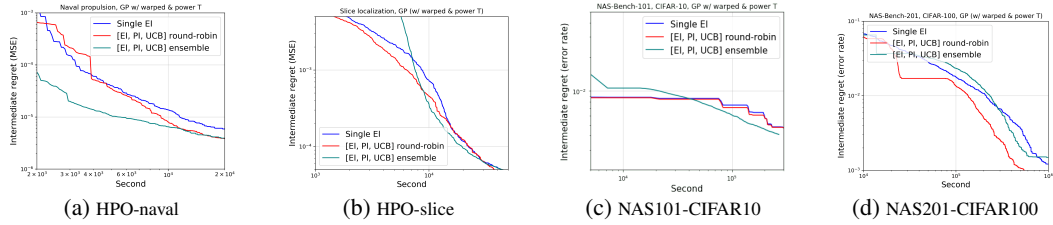


Figure S3. Comparison of mean intermediate regret performance r_t when a different acquisition strategy is used in a typical BO. Utilizing multiple acquisition functions can be performed in many different ways. Here, the simple round-robin strategy is based on Cho et al. [9] and the ensemble strategy is based on Cowen-Rivers et al. [14]. We also compare them with EI acquisition only [50], that is commonly used.

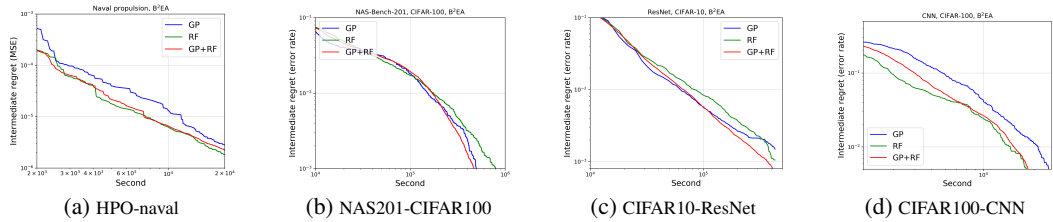


Figure S4. Comparison of mean intermediate regret performance r_t for three different choices of surrogate model in B^2EA (GP only, RF only, both GP and RF). We plotted the mean r_t values of 100 repeated runs. Traditionally, GP has been known to be effective for optimizing continuous variables and RF has been known to be effective for optimizing categorical variables. However, our experiment results over NAS tasks do not agree with the known wisdom. Therefore, we have chosen to use both GP and RF as the surrogate models in B^2EA .

E Success Rate $\mathbb{P}(\tau \leq t)$ Performance

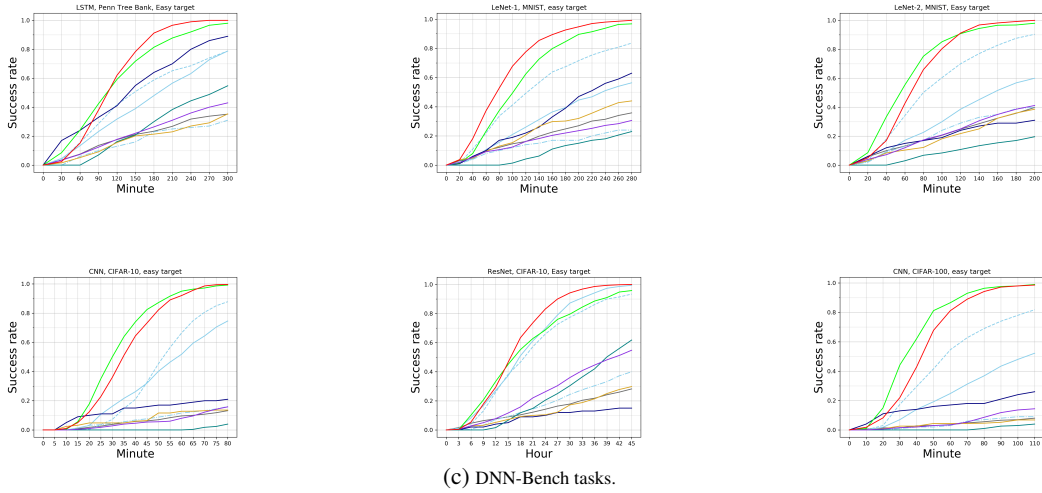
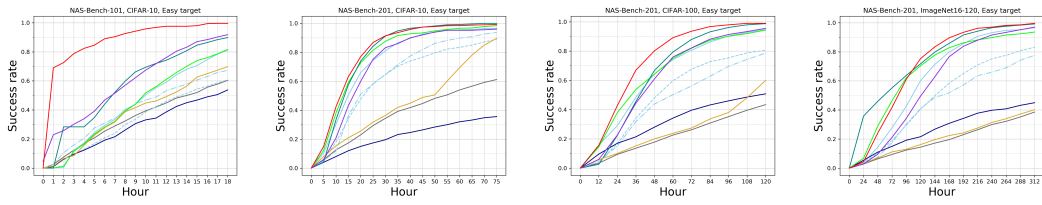
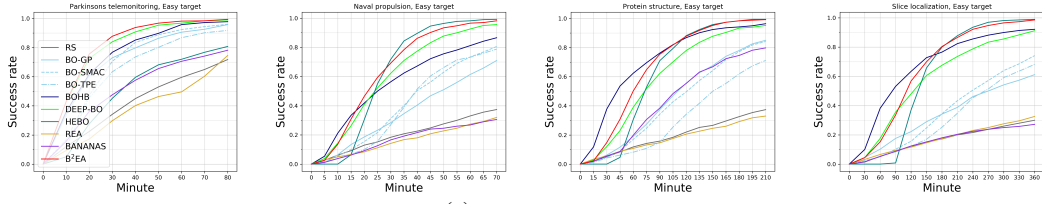
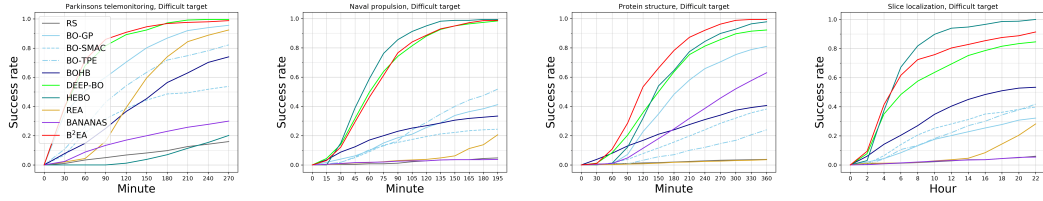
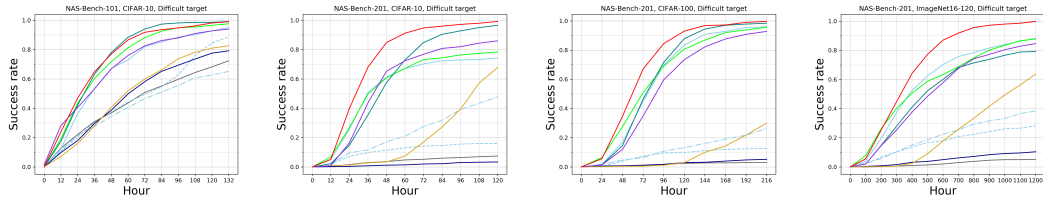


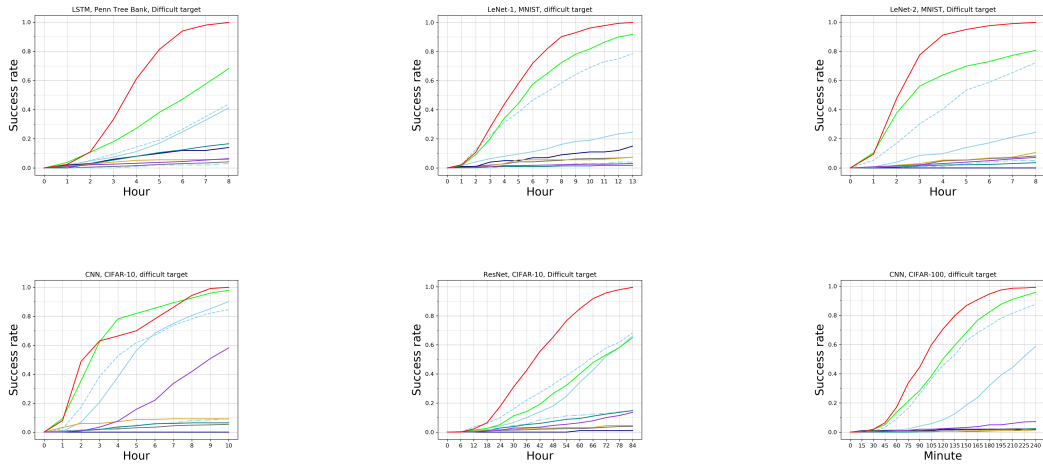
Figure S5. Comparison of the success rate for the easy target $\mathbb{P}(\tau \leq t_e)$, plotted with t as the horizontal axis.



(a) HPO-Bench tasks.

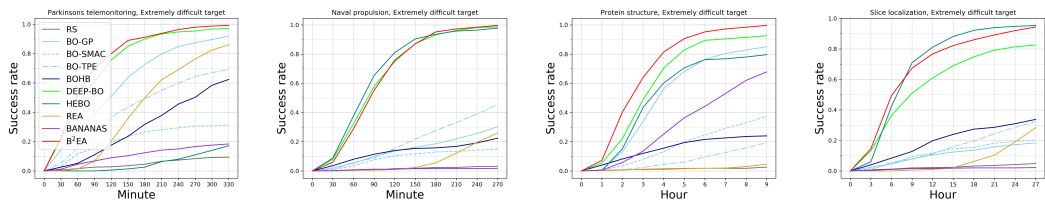


(b) NAS-Bench tasks.

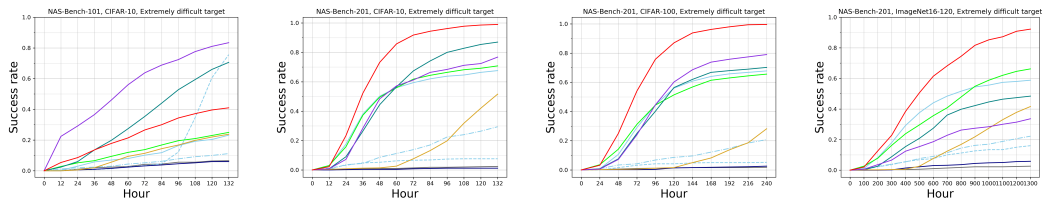


(c) DNN-Bench tasks.

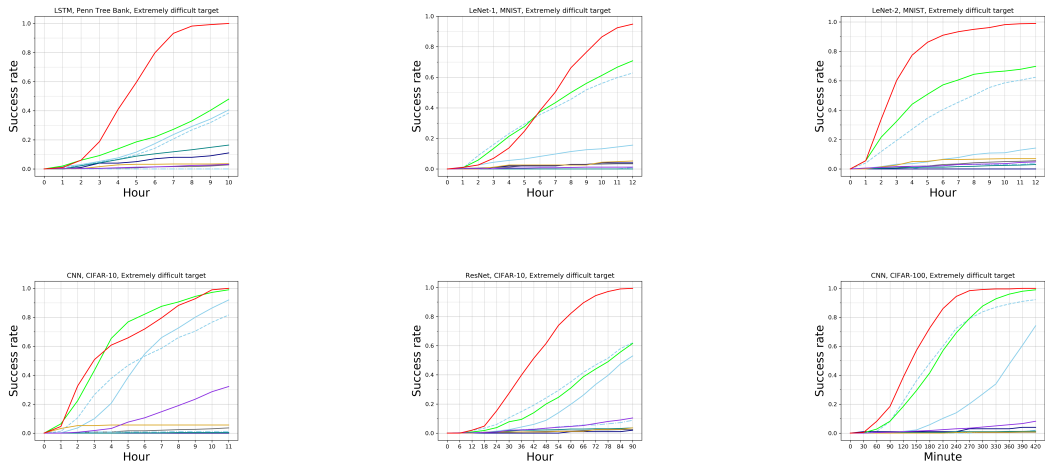
Figure S6. Comparison of the success rate for difficult target $\mathbb{P}(\tau \leq t_d)$, plotted with t as the horizontal axis.



(a) HPO-Bench tasks.



(b) NAS-Bench tasks.



(c) DNN-Bench tasks.

Figure S7. Comparison of the success rate for extremely difficult target $\mathbb{P}(\tau \leq t_x)$, plotted with t as the horizontal axis.